

Slot Synchronization of a WDM Packet-Switched Slotted Ring

Stefano Bregni, *Senior Member, IEEE*, Roberto Gaudino, *Member, IEEE*, Achille Pattavina, *Senior Member, IEEE*, Diego Carzaniga, and Alessandro Antonino

Abstract—In this paper, we present two different strategies of slot synchronization in wavelength-division-multiplexing (WDM) packet-switched slotted-ring networks. Emphasis is given to the architecture behind the WDM Optical Network Demonstrator over Rings (WONDER) project, which is based on tunable transmitters and fixed receivers. The WONDER experimental prototype is currently being developed at the laboratories of Politecnico di Torino. In the former strategy, a slot-synchronization signal is transmitted by the master station on a dedicated control wavelength; in the latter, slave nodes achieve slot synchronization aligning on data packets that are received from the master. The performance of both synchronization strategies, particularly in terms of packet-collision probability, was evaluated by simulation. The technique based on transmitting a timing signal on a dedicated control wavelength achieves better performance, although it is more expensive due to the need for an additional wavelength. However, the technique based on aligning data packets that are received from the master, despite attaining lower timing stability, still deserves further study, particularly if limiting the number of wavelengths and receivers is a major requirement. Some experimental results, which were measured on the WONDER prototype, are also shown. Measurement results, together with theoretical findings, demonstrate the good synchronization performance of the prototype.

Index Terms—Metropolitan-area networks (MANs), optical networks, phase-locked loops (PLLs), synchronization, wavelength-division multiplexing (WDM).

I. INTRODUCTION

WAVELENGTH-division-multiplexing (WDM) packet-switched ring architectures that are based on tunable transmitters and fixed receivers have sparked significant interest in the optical networking area [1], owing to their good balance between optical and electronic complexities [2], [3]. Such architectures have been studied under different aspects [4], [5] and applied in several experimental projects, such as HORNET [6] and RingO [7]. More recently, the WDM Optical Network

Demonstrator over Rings (WONDER) project [8], [9] has further developed the RingO design, with the ambitious goal of building and testing an experimental optical ring network that is capable of carrying real IP traffic.

These ring networks are based on synchronous time-slotted operation on all wavelengths, with a typical slot duration in the microsecond range. Similar architectures have already been analyzed under many aspects in several papers. Nevertheless, to our knowledge, possible techniques for the slot synchronization of such networks have not been investigated, and their performance has not been evaluated yet.

In the laboratories of Politecnico di Torino, the WONDER prototype is currently under experimental development. Among the various challenging tasks of this project, we have investigated possible time-slot synchronization techniques that are suitable for application in this project, as well as in similar networks.

In this paper, we report some of the most interesting results obtained in this work. We studied two different strategies of slot synchronization in these types of ring architectures, with emphasis on the WONDER network; in the former, a slot-synchronization signal is transmitted by the master station on a dedicated control wavelength; in the latter, slave nodes achieve slot synchronization aligning on data packets that are received from the master.

This paper is organized as follows. An essential review of the WONDER architecture is given in Section II. Section III presents the network model and the relevant assumptions. Sections IV and V detail the two synchronization techniques and report some performance evaluation results. Finally, Section VI presents some experimental results that were measured on the prototype system.

II. WONDER ARCHITECTURE

WONDER is a research project [8], [9] that is focused on demonstrating the feasibility of a ring packet-switched optical metropolitan-area network using state-of-the-art, but commercially available, optoelectronic technology. It is a development of the RingO design [7].

The WONDER network topology and node architecture are based on two fiber rings connecting N nodes, as shown in Fig. 1. One of the rings (TX) is devoted to data transmission, while the other (RX) is devoted to data reception. The WDM network is designed according to the tunable-transmitters/fixed-receivers paradigm [2], [4]. The transmission of packets is time-slotted and synchronized on all wavelengths. Each node

Manuscript received November 2, 2006; revised July 12, 2007. This paper is based, but not exclusively, on the paper "Slot Synchronization of WDM Packet-Switched Slotted Rings: The WONDER Project," by S. Bregni, D. Carzaniga, R. Gaudino, and A. Pattavina, which appeared in the *Proceedings of the IEEE ICC 2006*, Istanbul, Turkey, June 2006. This work was supported in part by Ministero dell'Istruzione, dell'Università e della Ricerca (MIUR), Italy, under PRIN Projects WONDER and OSATE, and in part by the European Union under the FP6 Network of Excellence e-Photon/ONe+.

S. Bregni, A. Pattavina, and D. Carzaniga are with the Department of Electronics and Information, Politecnico di Milano, 20133 Milano, Italy (e-mail: bregni@elet.polimi.it; pattavina@elet.polimi.it).

R. Gaudino and A. Antonino are with the Department of Electronics, Politecnico di Torino, 10129 Torino, Italy (e-mail: gaudino@polito.it).

Digital Object Identifier 10.1109/JLT.2007.904938

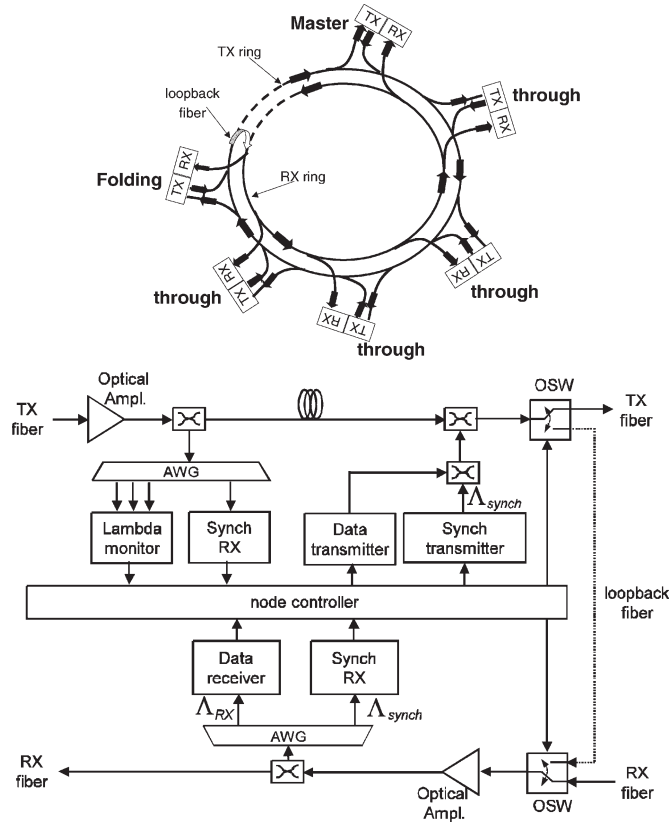


Fig. 1. WONDER network and node architecture.

has a “ Λ -monitor” capability on the TX fiber, which allows the sensing of the presence or absence of data signals (data packets) on each wavelength at every time slot. In short, nodes transmit data (optical bursts) on the TX fiber, on the wavelength of the destination node, and in a time slot found available by the Λ -monitor function. Therefore, nodes add their data packets on the TX fiber. On the other hand, data are received (read) on the TX fiber.

The two rings are physically interconnected through an optical shortcut that can be placed at any node. This shortcut, which is key to the WONDER fault-recovery capability [10], is realized by closing an optical loopback between the TX and RX rings at the output of a node. Thus, the resulting topology can also be viewed as a folded bus on which each node has two connections in two distinct points.

One wavelength may be dedicated to carry control signals (e.g., for fault protection [10] and physical-layer monitoring), service signals (e.g., for indicating slot reservation for synchronous data transfer), and, as studied in this paper, a bit/slot-synchronization signal.

Due to space limitations, only the main features of the network and node architecture can be outlined here. For further details on the network design and experimental activity, see [7], [9], [10].

As far as network synchronization is concerned, the most straightforward approach consists of distributing a timing signal on the dedicated wavelength. In this case, the first node of the folded bus (master node) transmits a periodic synchronization signal (e.g., pulses) on the control wavelength of the TX fiber,

while every other node receives this signal on the RX fiber. The slot-synchronization goal is enabling the transmitting nodes to insert packets ideally at the center of (empty) time slots. Misalignment on slot boundaries may ultimately lead to packet transmission on the border between adjacent time slots, thus leading to packet collisions and, finally, to data loss.

III. NETWORK MODEL AND ASSUMPTIONS

The network model is characterized by the following parameters:

- 1) number N of network nodes, numbered as $j = 1, 2, \dots, N$;
- 2) number W of data wavelengths used to transmit packet; since $N = W$ is assumed (i.e., every node uses a unique optical channel to receive data), node j receives packets only on the wavelength Λ_j ;
- 3) (ideal) time-slot duration T_S (in our simulations, we set $T_S = 1 \mu\text{s}$);
- 4) packet-transmission time $T_P = 0.9 \mu\text{s}$ (considered constant in each node and in each time slot, independent of node-clock error);
- 5) fiber length L between adjacent nodes;
- 6) delay fiber length l used in every node;
- 7) length F of the folding fiber used in the last node to link transmission and reception fibers;
- 8) wavelength spacing $\Delta\lambda = 0.8 \text{ nm}$;
- 9) chromatic-dispersion coefficient equal to $16 \text{ ps}/(\text{km}\cdot\text{nm})$ (i.e., 12.8 ps/km);
- 10) instant $t_{k,j}$ in which node j receives the signal indicating the beginning of k th time slot;
- 11) random time error (TE) $\text{TE}_{k,j}$ of the time-slot-synchronization signal [11]; this value represents the time difference between the ideal reference (pulses received deterministically every microsecond) and the real reference for node j at slot k .

Each node stores packets that are received from clients in a logical queue. The client-packet-arrival process is modeled as a Poisson process: Interarrival times at node i are exponentially distributed with an average rate of λ_i packets per slot. Client packets are sent to other nodes uniformly, with an average transmission rate of $R_{i,j}$ from node i to node j [in packets per slot]

$$R_{i,j} = \lambda_i \cdot \frac{1}{N-1}, \quad R_{i,i} = 0. \quad (1)$$

Distributing time-slot synchronization to network nodes as accurately as possible is a key objective. Every node is expected to know exactly the beginning of each time slot on both the TX and RX fibers. This information is not essential on the RX. In fact, nodes are capable of receiving packets with their burst-mode packet receiver, and this operation is possible without knowing that, in the next slot, a packet will arrive.

On the TX fiber, at the beginning of each time slot, nodes perform the following operations: 1) sampling the data channels (with the Λ -monitor function) in order to determine the idle or

busy condition of each wavelength for the transmission in that time slot and 2) transmission of a packet on one of the available wavelengths; the MAC is based on a proper queuing strategy.

The packet-transmission time has been chosen: $T_P = 0.9 \cdot T_S$. Thus, a guard time $T_G = 0.1 \cdot T_S$ is left to compensate for limited TE and chromatic dispersion.

Allowing a guard time does affect the Λ -monitor operation. In fact, sampling the data channel too soon (just after the slot start) makes it highly probable for the optical power on one or more wavelengths not to be detected due to TE and chromatic dispersion. This can lead to an erroneous detection of one or more wavelengths as idle, in spite of them being actually busy, thus causing a collision when these wavelengths are used by the node for packet transmission.

In order to avoid these collisions, every node has to sample data channels with a certain delay (channel-probing delay, D_p) after the beginning of the time slot. If every node samples data channels at the middle of the time slot, i.e., $D_p = 0.5 \mu s$ (the assumption used in our entire study), the probability of avoiding detection errors due to TE and chromatic dispersion is minimized. However, this yields an additive delay of half a time slot, as well as the need for a longer fiber delay line in each station (used also to take into account the unavoidable electronic processing time of MAC operations).

In the next sections, two different time-slot-synchronization techniques for the WONDER ring are described. In the former, a slot-synchronization signal is transmitted by the master station on a dedicated control wavelength. In the latter, slave nodes achieve slot-synchronization aligning on data packets that are received from the master. For both of these, the performance has been evaluated by simulation and then by outlining advantages and drawbacks.

IV. SYNCHRONIZATION SIGNAL TRANSMITTED ON DEDICATED CONTROL WAVELENGTH

In this case, $W + 1$ wavelengths are used: $W = N$ data channels and one additional dedicated channel to carry the synchronization signal. In this scenario, the first node on the transmission fiber is the master node. It transmits a timing signal that propagates along the fiber, indicating to all other stations the start of time slots. Every slave node needs to receive this slot-synchronization signal: Thus, the generic node j has a receiver not only for wavelength Λ_j (on the RX fiber) but also for control wavelength Λ_C (on the TX fiber).

A. System Model Basics

Ideally, the signal transmitted from the master on Λ_C is a series of pulses spaced at $1 \mu s$ from each other, which is detected by every station without timing error. Hence, no collisions happen. In a real scenario, on the contrary, several impairments can take place: The master station clock is subject to phase and frequency deviations [11]; the generic slave node probes the received signal and begins packet transmission a bit sooner or a bit later than expected, and the processing time required by MAC operations is different from that added by the fiber delay line. These effects contribute to make network nodes

affected by TE and to make packet collisions more frequent due to time-slot misalignment.

In addition, chromatic dispersion plays an important role in slot synchronization, as it causes packets that are transmitted on different wavelengths to propagate at different speeds. For this reason, packets transmitted on different wavelengths arrive to a destination that deviates from ideal time alignment. In order to reduce the negative effects of chromatic dispersion, the control wavelength is placed as a ‘‘central wavelength’’ between data channels, with the propagation speed assumed to be $\nu = 2 \cdot 10^8$ m/s.

Given the parameters defined previously, we can express the slot-synchronization time $t_{k,j}$ at node j for slot k as

$$t_{k,j} = kT_S + (j - 1) \cdot \frac{(L + l)}{\nu} + TE_{k,j}. \quad (2)$$

The term $(j - 1)(L + l)/\nu$ is the propagation delay. $TE_{k,j}$ is the random TE that, combined with chromatic dispersion, may cause packet collision. In all simulations, the effect of chromatic dispersion has been taken into account, although not explicitly indicated in this and the following formulas.

In our model, $TE_{k,1}$ is the random TE series of the first clock in the chain, i.e., the master node. As far as the other nodes ($j > 1$, slave nodes) are concerned, we considered two possibilities: 1) a simple model, in which each slave node simply detects pulses on the control wavelength, which are affected by random trigger error, and 2) a phase-locked loop (PLL) model, in which slave clocks behave as a PLL that tracks the timing signal transmitted by the master.

B. Simple Model

In the simple model, we have the following assumptions.

- 1) In a given time slot k , the values $TE_{k,j}$ are independent (i.e., TE samples in the same time slot at different nodes are uncorrelated).
- 2) In a given node j , the values $TE_{k,j}$ are independent (i.e., no time correlation is assumed in TE sequences at every node).
- 3) The random variables $TE_{k,j}$ have uniform probability distribution in the interval $(-\sqrt{3}\sigma, +\sqrt{3}\sigma)$, where σ is the distribution standard deviation.

C. PLL Model

In the PLL model, the slave node PLL low-pass filters phase fluctuations of the synchronization signal on the control wavelength [11]. PLL internal noise comes mainly from two sources: the voltage-controlled oscillator (VCO) and the phase detector and loop filter [11], [12]. The former noise is high-pass filtered to the output signal, whereas the latter is low-pass filtered. We neglected the VCO noise because quartz oscillators are very stable in the short term. On the other hand, we modeled the phase-detector and loop-filter noise by the random TE series $TE_{k,j}^{DF}$, where we have the following assumptions.

- 1) In a given time slot k , the values $TE_{k,j}^{DF}$ are independent.
- 2) In a given node j , the values $TE_{k,j}^{DF}$ are independent.

- 3) The random variables $TE_{k,1}$ have uniform probability distribution in $(-\sqrt{3}\sigma_M, +\sqrt{3}\sigma_M)$, where σ_M is the standard deviation of the random TE on the master clock.
- 4) The random variables $TE_{k,j}^{DF}$ have a uniform probability distribution in $(-\sqrt{3}\sigma_{DF}, +\sqrt{3}\sigma_{DF})$, where σ_{DF} is the standard deviation of the random TE generated at the PLL phase detector and loop filter.

The second and fourth assumptions reflect what may be expected from a digital PLL with a quantizerlike phase detector.

We assumed the classic linear baseband model of a second-order PLL with an active loop filter (perfect integrator) [11], which has an input–output phase-transfer function

$$H(s) = \frac{\phi_{OUT}(s)}{\phi_{IN}(s)} = \frac{2\zeta\omega_N s + \omega_N^2}{s^2 + 2\zeta\omega_N s + \omega_N^2} \quad (3)$$

where ζ is the damping ratio (we assumed that $\zeta = 1$), and ω_N is the natural angular frequency. We remark that, in the PLL linear model (3), the cutoff (-3 -dB point) frequency B is proportional to its natural frequency $f_N = \omega_N/2\pi$, as

$$B = \frac{\omega_N}{2\pi} \sqrt{2\zeta^2 + 1 + \sqrt{(2\zeta^2 + 1)^2 + 1}}. \quad (4)$$

With $\zeta = 1$, we have $B \cong 2.48 \cdot f_N$.

Therefore, the TE series at each node j is given by

$$TE_{k,j} = \begin{cases} TE_{k,1}, & j = 1 \\ TE_{k,1} * h(k) + TE_{k,j}^{DF} * h(k), & j = 2, 3, \dots, N \end{cases} \quad (5)$$

where $h(k)$ is the impulse response corresponding to $H(s)$.

D. Performance Evaluation

We have evaluated the network performance of both the simple and PLL models for different values of the clock-noise standard deviations σ_{DF} and σ_M and of the natural frequency f_N . All simulations have been run repeatedly and independently until 95% confidence intervals, which is less than 5% of the collision-probability estimate, were attained. The discrete-event simulator was realized in OMNeT++ [13].

Fig. 2 plots the packet-collision probability (averaged on all nodes) as a function of σ_M , with the timing signal on a dedicated control wavelength, with and without a PLL in each node ($\sigma_{DF} = 1$ ns), and with uniform packet-arrival rate $\lambda_i = 0.9$ packets/slots. Mostly, using PLLs improves network performance, particularly when B is sufficiently low. Nevertheless, we observed that the simple model may achieve better performance in some cases, i.e., when B is high and the TE standard deviation σ_M of the master node is low. Moreover, while the collision probability decreases with B for small σ_M , the opposite behavior is observed for high values of σ_M . This is caused by the velocity at which PLLs follow input-phase fluctuations: If B is high, this velocity is high, although internal noise is not filtered out much. For high input noise, this last phenomenon prevails and yields lower collision probability.

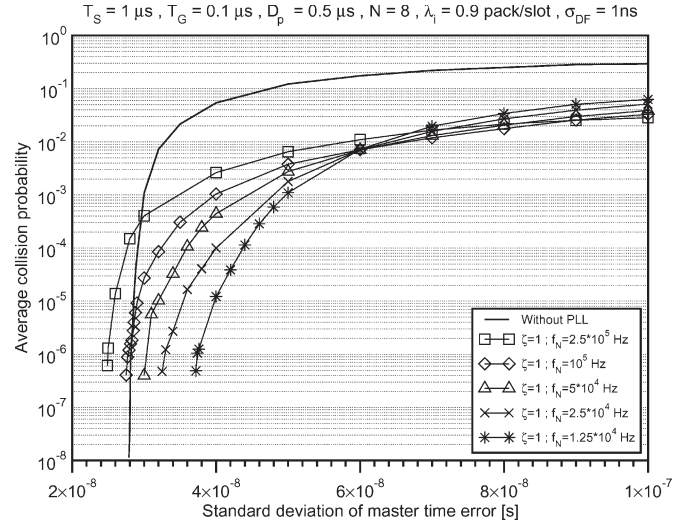


Fig. 2. Collision probability averaged on all nodes as a function of σ_M ($\sigma_{DF} = 1$ ns), with a timing signal on a dedicated control wavelength (simple model and PLL model).

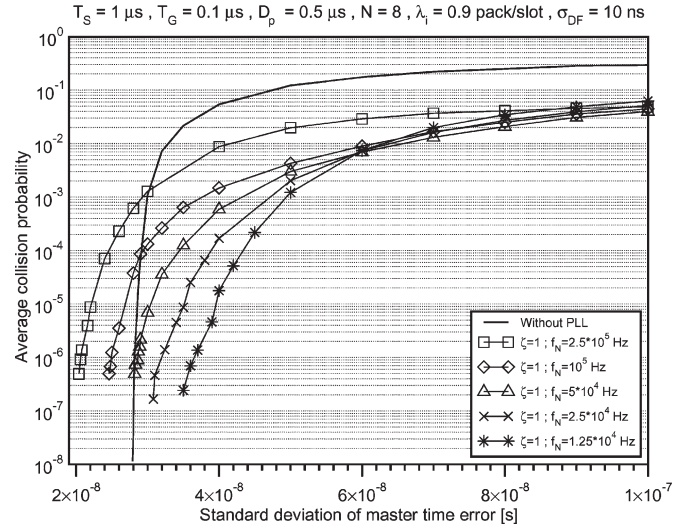


Fig. 3. Collision probability averaged on all nodes as a function of σ_M ($\sigma_{DF} = 10$ ns), with a timing signal on a dedicated control wavelength (simple model and PLL model).

The actual performance improvement of the PLL-based synchronization solution depends on the amount of PLL internal noise σ_{DF} . Fig. 3 shows analogous simulation results as Fig. 2 but obtained for $\sigma_{DF} = 10$ ns. Compared to Fig. 2, PLL-based curves are shifted to the left, thus making the solution without PLL more convenient in a larger range of network parameters, particularly for higher values of the PLL natural frequency.

The design of a network with a PLL in each slave node would require knowing the maximum standard deviation of the master node TE (σ_M) and of the PLL internal TE (σ_{DF}) that can be tolerated, in order to have a collision probability lower than a given limit. Figs. 4 and 5 provide such information for given values of the collision probability P_C and of the PLL natural frequency f_N .

Fig. 4 shows that TE requirements are more severe with a higher PLL cutoff frequency B . The lower B is, the more the noise power is filtered out, and thus, the working area in

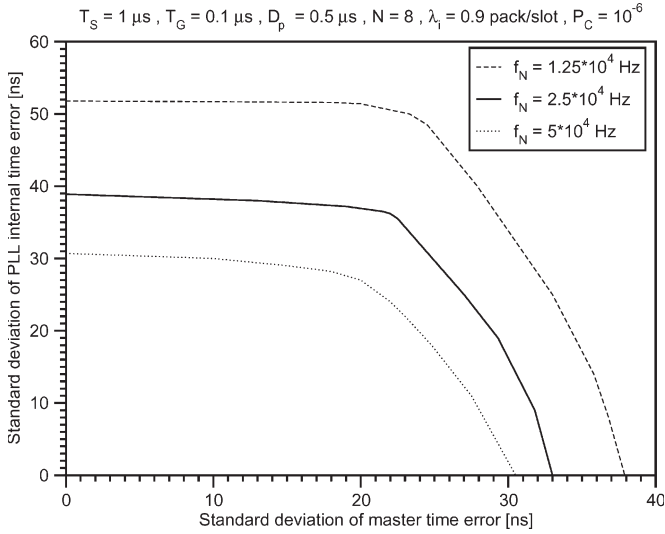


Fig. 4. Loci of the standard deviations σ_M (noise from master clock) and σ_{DF} (noise from PLL phase detector and loop filter) with the same collision probability $P_C = 10^{-6}$ and PLL natural frequency f_N .

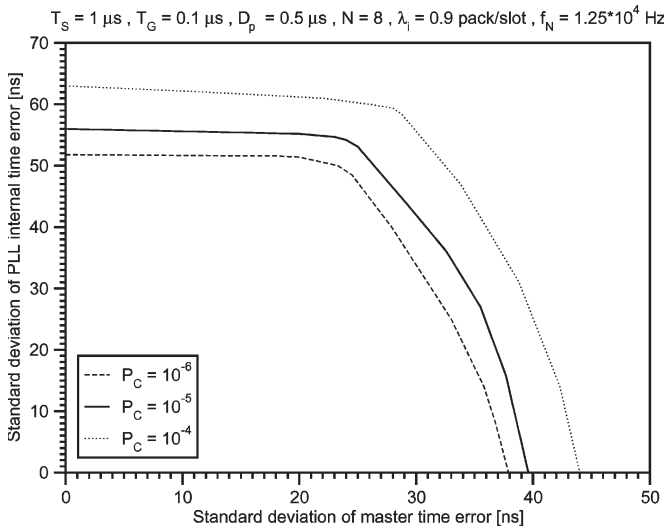


Fig. 5. Loci of the standard deviations σ_M (noise from master clock) and σ_{DF} (noise from PLL phase detector and loop filter) with the same collision probability P_C and PLL natural frequency $f_N = 12.5$ kHz ($B \cong 31$ kHz).

the graph (below the curve) becomes bigger. Moreover, both Figs. 4 and 5 exhibit asymmetry of curves. The random TE of the master node adversely affects the collision probability, more than the random TE in the PLL phase detector and loop filter. This asymmetry vanishes if f_N is high (e.g., 50 kHz). From Fig. 5, we can also note that the asymmetry of curves is larger for a higher collision probability.

V. SYNCHRONIZATION ON DATA PACKETS FROM THE MASTER

Slot synchronization based on transmitting a timing signal on a dedicated control wavelength, although granting good performance, has two important drawbacks: 1) the need for one additional wavelength and 2) the need for need of one additional receiver on the TX fiber in every node (except the master).

Thus, in order to reduce the network cost, we envisaged an alternative slot-synchronization technique based on aligning on the arrival times of data packets that are transmitted by the master. In this method, it is assumed that, in each node, the fixed delay from the slot on the TX and the slot on the RX is known.

A. System Model

In this scenario, the master node is not necessarily the first node on the TX fiber. The master is assumed to have an ideal clock, which chimes time slots every microsecond and triggers the transmission of data packets. When a node receives a packet from the master (the packet header includes sender information), it determines the beginning of the next slot on the TX fiber adding the fixed delay and some unavoidable TE because of it is based on the local inaccurate clock and nonideal detection. However, let us point out that slave nodes do not receive a packet from the master at every slot: When they do not, they evaluate the next slot start time on the TX based on their inaccurate clock. Now, we remark that 1) slave nodes get synchronized by the arrival of data packets from the master; on packet arrival, they align their clock phase to the master clock, not necessarily in the next slot but possibly in one of the following slots, if delay from reception to transmission is too short, and 2) the contribution of chromatic dispersion can be estimated in advance and used to correct clock realignment after the reception of data packets.

To model slot synchronization on data packets from the master, two vectors have been defined: 1) $\mathbf{r}_j^M = \{r_{i,j}^M\}$ time instants in which node j receives packet i from the master ($j = 1, 2, \dots, N; i = 1, 2, \dots$) and 2) $\mathbf{t}_j^M = \{t_{i,j}^M\}$ time instants in which node j schedules the beginning of time slot i on the TX, based on the timing of data packets received from the master ($j = 1, 2, \dots, N; i = 1, 2, \dots$).

The start instant of time slots is computed by the generic slave node j (node 1 identifies the master) as

$$t_{k,1} = kT_S \tag{6}$$

$$t_{0,j} = t_{1,j}^M + TE_{0,j} \tag{7}$$

$$t_{k,j} = t_{i,j}^M + TE_{k,j} \tag{8}$$

$$\text{if } \exists i \mid t_{k-1,j} \leq r_{i,j}^M < t_{k-1,j} + T_S + TE_{k,j} \tag{8}$$

$$t_{k,j} = t_{k-1,j} + T_S + TE_{k,j} \tag{9}$$

$$\text{if } \nexists i \mid t_{k-1,j} \leq r_{i,j}^M < t_{k-1,j} + T_S + TE_{k,j} . \tag{9}$$

We point out that, here, slot numbering is not global, like in (2), because, for each node, the first slot begins after reception of the first packet from the master. The formulas above mean the following (the fixed delay between nodes has not been indicated explicitly).

- 1) The master has an ideal clock (6).
- 2) Each node waits for the first packet from the master to begin transmission (7).
- 3) When a node receives a packet from the master, it determines the next transmission instant, adding the fixed delay between slots on the TX and RX fibers and some

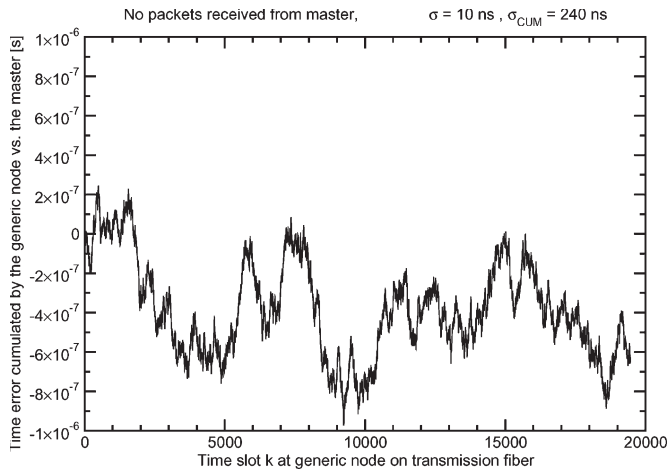


Fig. 6. Cumulative TE in a slave node ($\sigma = 10$ ns), with no data packets from the master ($\lambda_M = 0$ packets/slot).

TE because it is based on the local inaccurate clock and nonideal detection (8).

- 4) When a node does not receive a packet from the master, it determines the beginning of the next time slot on the TX fiber using its inaccurate internal clock (9).

B. Performance Evaluation

It is evident that network synchronization performance depends strongly on the average rate λ_M , with which packets are received from the master. To verify it, this synchronization method has been simulated over 20 000 time slots, according to relationships (6)–(9). For the sake of simplicity, $TE_{k,j}$ samples have been assumed to be uncorrelated and distributed uniformly in interval $(-\sqrt{3}\sigma, +\sqrt{3}\sigma)$, first setting their standard deviation to $\sigma = 10$ ns.

Under this simple assumption, if the slave node can never align on data packets received from the master (i.e., $\lambda_M = 0$), its cumulated TE wanders without limit. This result, based on the random process theory, is called random walk (i.e., integral of white noise), which is the continuous summation of independent increments (random TE samples).

Fig. 6 shows the cumulated TE sequence in a generic slave node, obtained by simulation for $\lambda_M = 0$. The standard deviation of this finite sequence results in $\sigma_{CUM} = 240$ ns. Note that the variance of a random walk, which is defined by infinite-time averaging, is infinite. Thus, the value σ_{CUM} actually depends on the sequence length.

The more often a node can align its time scale on the arrival times of data packets from the master, the lower the standard deviation of its cumulated TE will be. For example, Figs. 7 and 8 show the TE cumulated by the slave node when $\lambda_M = 0.1$ ($\sigma_{CUM} = 84$ ns) and $\lambda_M = 0.9$ ($\sigma_{CUM} = 29$ ns).

Fig. 9 plots the packet-collision probability (averaged on all nodes) as a function of σ , which is measured in the three cases of Figs. 6–8, as compared with that achieved by synchronization on a dedicated control wavelength (simple model). The collision probability apparently decreases with an increase in λ_M . However, we note that the synchronization technique based on a dedicated control wavelength performs better than the

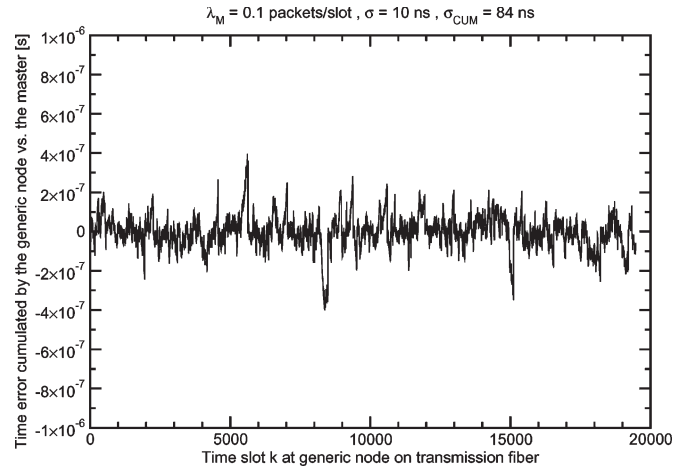


Fig. 7. Cumulative TE in a slave node ($\sigma = 10$ ns), aligning on data packets from the master ($\lambda_M = 0.1$ packets/slot).

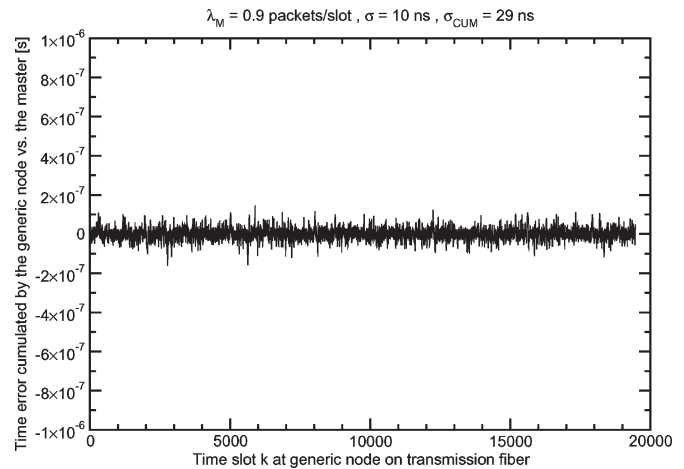


Fig. 8. Cumulative TE in a slave node ($\sigma = 10$ ns), aligning on data packets from the master ($\lambda_M = 0.9$ packets/slot).

method of synchronizing on data packets from the master, with all λ_M values considered.

Finally, simulation results shown in Fig. 10 illustrate how the number of network nodes affects performance, considering these three cases: $N = 8, 16,$ and 32 nodes, with $\lambda_M = 0.9$. As expected, the packet-collision probability increases with the number of nodes for any given σ . In fact, increasing the number of nodes implies that each node receives packets from the master less frequently. Hence, the cumulated TE in slave nodes becomes larger.

VI. EXPERIMENTAL SETUP AND MEASUREMENT RESULTS

In the current experimental WONDER testbed [8]–[10], synchronization is distributed through a dedicated wavelength, over which an NRZ 8B/10B encoded signal at 125 Mb/s is transported (thus using the typical 100 Base-FX Fast-Ethernet modulation). This control signal, which is generated by the master node and received by all slave nodes, enables the following functions.

- 1) Each slave node, using a standard (continuous) clock-and-data-recovery circuit, can recover the 125-Mb/s

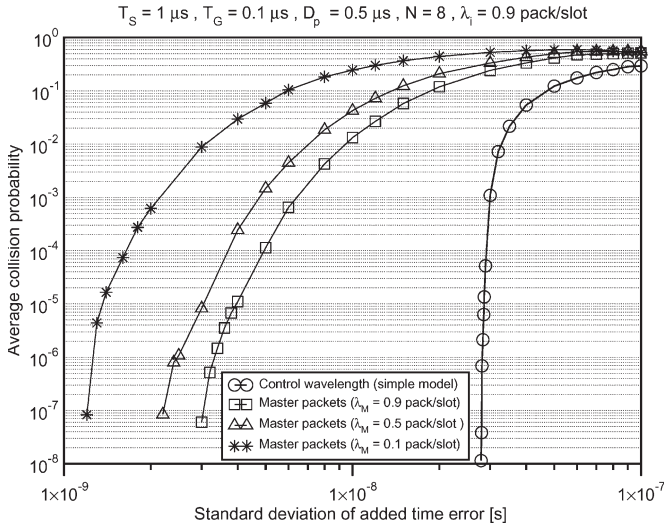


Fig. 9. Collision probability averaged on all nodes as a function of σ , with synchronization on data packets from the master, compared to synchronization on dedicated control wavelength.

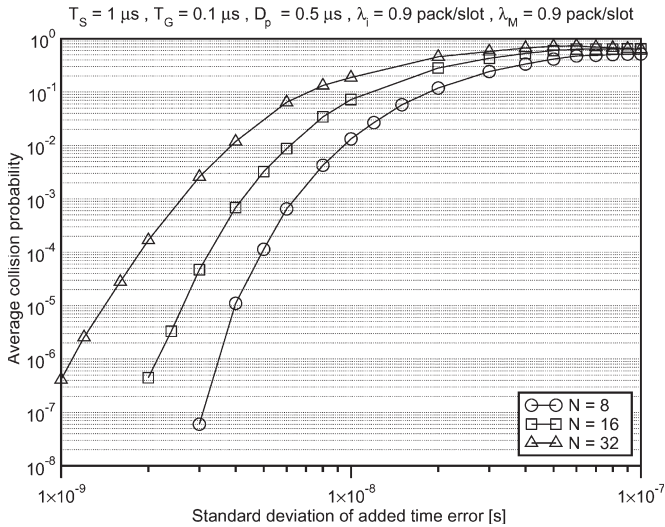


Fig. 10. Collision probability was averaged on all nodes as a function of σ , with synchronization on data packets from the master ($\lambda_M = 0.9$), compared for different numbers of network nodes: $N = 8, 16,$ and 32 .

signal and derive a precise 125-MHz reference clock, which is frequency locked to the master-node clock. This way, all nodes are synchronized by this common 125-MHz reference, aiding burst-mode operation for the high-speed transmission at 1.25 Gb/s, as detailed in [14].

- 2) The control signal provides a “signaling path” from the master node to all slave nodes.
- 3) Slave nodes can sense any fiber cut in the ring by simply monitoring the control signal. Fault-recovery mechanisms are thus allowed, as detailed in [10].
- 4) Most relevant to this paper, a suitably placed 8 B/10 B control word in the 125-Mb/s data stream indicates the beginning of each time slot, thus distributing the slot-synchronization time $t_{k,j}$ [see (2)].

In the following, we present some experimental results measured on the WONDER prototype system, and we compare them to the simulation results shown in previous sections.

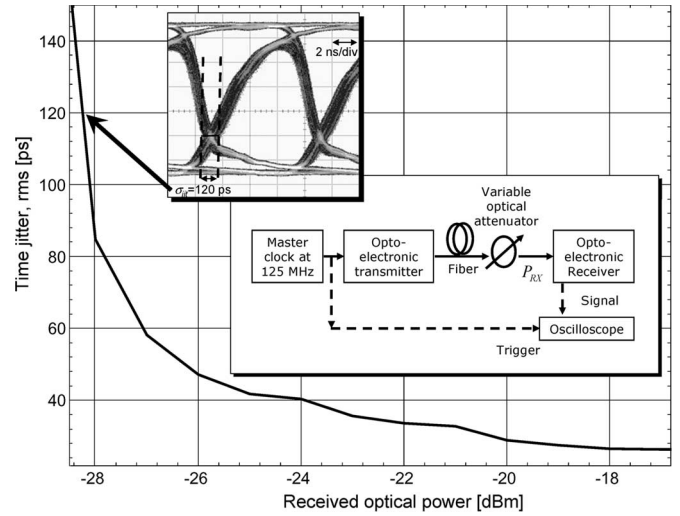


Fig. 11. Measured jitter on the recovered synchronization signal at the master node versus received optical power (no ASE noise). Insets show the measurement setup and, as an example, the received eye diagram in the case of a 120-ps (rms) jitter.

Let us consider first the accuracy of the master-node time base. In our system, this time is generated in a high-performance field programmable gate array (FPGA). Its timing quality is affected by two contributions: 1) the jitter generated by the FPGA circuits. In the FPGA datasheet, the jitter amplitude on any output signal is specified to be less than 500 ps (rms). In the following, we will refer to these values as FPGA intrinsic jitter. 2) the frequency accuracy and the output jitter of the FPGA internal quartz oscillator. The datasheet specifies the former as $2.5 \cdot 10^{-5}$ (maximum fractional frequency error) and the latter as 2.5 ps (rms), which is clearly negligible with respect to the FPGA intrinsic jitter.

Consequently, we can estimate the amplitude of the master-node total time jitter as 500 ps (rms). By inspection of Figs. 2 and 3, it can be noted that the master-node TE σ_M yields a negligible system penalty when it is below 20 ns. It can be concluded that the actual 500-ps master-node jitter of our experimental setup does not affect system performance.

Let us consider then the time accuracy in slave nodes. Here, a standard optical receiver at 125 Mb/s detects the synchronization wavelength and passes the resulting signal to the FPGA. Its accumulated jitter depends on the received optical power (when ASE noise is negligible) or on the received optical-signal-to-noise ratio (OSNR) when optical amplifiers are used. Thus, we measured signal jitter in both cases by simply using a standard function of the oscilloscope.

The standard deviation σ of the measured jitter, as a function of the received optical power, is plotted in Fig. 11. Jitter amplitude is well below 50 ps for any received power not less than -26 dBm, while it increases sharply for lower power levels. Similarly, the measured jitter versus OSNR is plotted in Fig. 12 and results well below 50 ps for any received OSNR above 12 dB. Both conditions ($P_{RX} \geq -26$ dBm, OSNR > 12 dB) are easily met in the WONDER experimental setup. For instance, the OSNR should be higher than ~ 17 dB to achieve the correct reception of the 1.25-Gb/s signal. Thus, under any reasonable operating conditions, the time jitter on the received

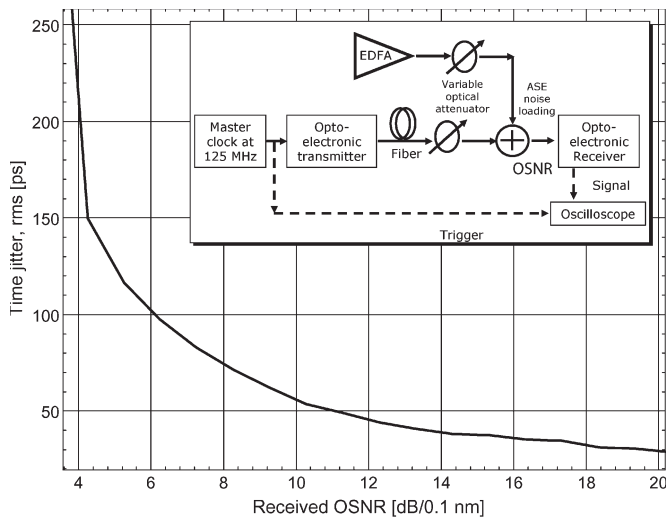


Fig. 12. Measured jitter on the recovered synchronization signal at the master node versus received OSNR. The inset shows the measurement setup.

synchronized signal is below 50 ps, which is well below the intrinsic 500-ps jitter of the FPGA circuits that will handle this signal. Therefore, we also conclude that, in the slave nodes, the resulting TE is, at worst, in the order of 500 ps. By inspection of the simulation results shown in Fig. 9, it appears again that any jitter amplitude $\sigma < 20$ ns yields negligible system penalty.

All these experimental measurements, coupled with the theoretical investigations described in the previous sections, allow us to draw an important conclusion: In the typical WONDER setup operating conditions, the TE of network signals is limited only by the FPGA intrinsic jitter. Moreover, measured or estimated values do not impact the overall network performance in practice.

VII. CONCLUSION

In this paper, two different strategies of slot synchronization in WDM packet-switched slotted-ring networks have been studied: In the former, a slot-synchronization signal is transmitted by the master station on a dedicated control wavelength; in the latter, slave nodes achieve slot synchronization aligning on data packets that are received from the master. Emphasis has been given to the architecture of the WONDER network, which is currently under experimental development. The performance of both synchronization strategies, particularly in terms of packet-collision probability, was evaluated by simulation. The technique based on transmitting a timing signal on a dedicated control wavelength was found to achieve better performance, particularly if every node tracks the timing reference by means of a PLL, which low-pass-filters the phase fluctuations on the timing signal transmitted by the master node.

Alternatively, aligning on data packets from the master allows savings in the cost of the additional control wavelength and associated receivers. Nevertheless, this technique was found to attain worse slot-synchronization performance. Each node is timed by the internal inaccurate clock in between master-packet arrivals. Therefore, the synchronization perfor-

mance is strongly dependent on the master-packet-transmission rate. However, this technique, although attaining lower timing stability, still deserves further study, particularly if limiting the number of wavelengths and receivers is a strong requirement.

In the WONDER experimental prototype, dedication of a wavelength channel to synchronization distribution has been chosen. Dedicating a wavelength for service purposes allows a variety of additional functions, such as the support of fault protection, indication of slot allocation for synchronous data transfer, and detection of faults. Moreover, a more complex synchronization signal may be transmitted on this control channel, distributing not only slot timing but also bit frequency, to aid burst-mode receivers in bit-timing acquisition.

By experimental measurements on the prototype, we have demonstrated that the synchronization system currently under test introduces TE values well below (by two orders of magnitude) the critical limits identified by simulation of the theoretical model.

All these results have been useful in the practical design of the WONDER network. They also spark general interest, since optical packet-switched slotted-ring networks have drawn significant attention to optical networking research.

REFERENCES

- [1] B. Mukherjee, *Optical Communication Networks*. New York: McGraw-Hill, 1997.
- [2] C. S. Jelger and J. M. H. Elmirghani, "Photonic packet WDM ring networks architecture and performance," *IEEE Commun. Mag.*, vol. 40, no. 11, pp. 110–115, Nov. 2002.
- [3] M. Herzog, M. Maier, and M. Reisslein, "Metropolitan area packet-switched WDM networks: A survey on ring systems," *Commun. Surveys Tuts.*, vol. 6, no. 2, pp. 2–20, 2nd Quarter 2004.
- [4] M. Ajmone Marsan, A. Bianco, E. Leonardi, M. Meo, and F. Neri, "MAC protocols and fairness control in WDM multi-rings with tunable transmitters and fixed receivers," *J. Lightw. Technol.*, vol. 14, no. 6, pp. 1230–1244, Jun. 1996.
- [5] H.-S. Yang, M. Herzog, M. Maier, and M. Reisslein, "Metro WDM networks: Performance comparison of slotted rings and AWG star networks," *IEEE J. Sel. Areas Commun.*, vol. 22, no. 8, pp. 1460–1473, Oct. 2004.
- [6] K. V. Shrikhande, I. M. White, D. Wonglumsom, S. M. Gemelos, M. S. Rogge, Y. Fukashiro, M. Avenarius, and L. G. Kazovsky, "HORNET: A packet-over-WDM multiple access metropolitan area ring network," *IEEE J. Sel. Areas Commun.*, vol. 18, no. 10, pp. 2004–2016, Oct. 2000.
- [7] A. Carena, V. De Feo, J. Finochietto, R. Gaudino, F. Neri, C. Piglione, and P. Poggiolini, "RingO: An experimental WDM optical packet network for metro applications," *IEEE J. Sel. Areas Commun.*, vol. 22, no. 8, pp. 1561–1571, Oct. 2004.
- [8] "PRIN Programme 2003," *Project WONDER (WDM Optical Network Demonstration Over Rings)*. Partners: Polytechnic of Turin, Polytechnic of Milan, University of Parma.
- [9] A. Bianciotto and R. Gaudino, "WONDER: Overview of a packet-switched MAN architecture," in *Proc. OpNeTec*, Pisa, Italy, Oct. 2004.
- [10] A. Bianciotto, J. Finochietto, R. Gaudino, F. Neri, C. Piglione, and A. Samperi, "Fast and efficient fault-recovery strategies in the WONDER metro architecture," in *Proc. NOC*, London, U. K., Jul. 2005.
- [11] S. Bregni, "Characterization and modelling of clocks," in *Synchronization of Digital Telecommunications Networks*. Chichester, U.K.: Wiley, 2002, pp. 203–281, ch. 5.
- [12] V. F. Kroupa, "Noise properties of PLL systems," *IEEE Trans. Commun.*, vol. COM-30, no. 10, pp. 2244–2252, Oct. 1982.
- [13] *OMNeT++ Discrete Event Simulation System*. [Online]. Available: <http://www.omnetpp.org>
- [14] A. Antonino, R. Birke, V. De Feo, J. M. Finocchietto, R. Gaudino, A. La Porta, F. Neri, and M. Petracca, "The WONDER testbed: Architecture and experimental demonstration," in *Proc. ECOC*, Berlin, Germany, Sep. 2007.



Stefano Bregni (M'93–SM'99) was born in Milano, Italy, in 1965. He received the degree in telecommunications engineering from Politecnico di Milano, in 1990.

From 1991 to 1993, he was with SIRTI S.p.A, and from 1994 to 1999, was with CEFRIEL Consortium, where he worked on synchronous digital hierarchy (SDH) and network-synchronization issues, specializing in clock-stability measurement. He served on the ETSI and ITU-T committees on digital network synchronization. In 1999, he was

tenured as an Assistant Professor and, since 2004, as an Associate Professor with Politecnico di Milano, where he has been teaching telecommunications networks. He is the author of about 50 papers, mostly in IEEE conferences and journals, and of the books *Synchronization of Digital Telecommunications Networks* (Chichester, U.K.: Wiley, 2002; translated and published in Russian by MIR, Moscow, Russia, 2003) and *Sistemi di trasmissione PDH e SDH—Multiplazione* (PDH and SDH Transmission Systems—Multiplexing. Milano, Italy: McGraw-Hill, 2004). His current research interests focus mainly on traffic modeling and optical networks.

Prof. Bregni is a Distinguished Lecturer of the IEEE Communications Society. He is the Vice Chair of the Transmission, Access, and Optical Systems Technical Committee and a voting member of the Globecom/ICC Technical Content Committee of the IEEE Communications Society. He is the Symposia Chair of IEEE Globecom 2009, the Symposium Chair of six other IEEE Globecom and ICC conferences, and the Workshop Chair of IEEE CCNC 2008. He is an Associate Editor of *IEEE Communications Surveys and Tutorials*. He was Tutorial Lecturer for four IEEE Globecom and ICC conferences.



Roberto Gaudino (M'99) was born in Torino, Italy, on August 9, 1968. He received the Ph.D. degree from Politecnico di Torino, Torino.

He spent one year in 1997 at the Georgia Institute of Technology, Atlanta, as a Visiting Researcher with the OCPN group, where he worked on the realization of the MOSAIC optical-network testbed. In 1998, he spent two years with the team that coordinates the development of the commercial optical-system simulation software OptSim. He is currently an Associate Professor with the Optical

Communication Group, Politecnico di Torino, where he works on several research topics related to optical communications. His main research interests are in the metro and long-haul dense-wavelength-division multiplexing systems, fiber nonlinearity, modeling of optical-communication systems, and on the experimental implementation of optical networks. Currently, he is investigating new optical modulation formats, such as polarization or phase modulation, and packet-switched optical networks. He is the author or coauthor of more than 80 papers in the field of optical-fiber transmission and optical networks. He is continuously involved in consulting for several companies of the optical sector and is also involved in continuing professional education. He is currently the Coordinator of the EU STREP Project "POF-ALL" and WP-Leader of the EU NOE "E-PhotonOne+."



Achille Pattavina (M'85–SM'93) received the Dr. Eng. degree in electronic engineering from University "La Sapienza," Rome, Italy, in 1977.

He was with University "La Sapienza" until 1991. He then moved to Politecnico di Milano, Milano, Italy, where he is currently a Full Professor. He is the author of more than 100 papers in the area of communications networks published in leading international journals and conference proceedings. He was a Guest or Coguest Editor of Special Issues on switching architectures in IEEE and non-IEEE

journals. He has been engaged in many research activities, including European Union-funded projects. His current research interests are in the area of optical networks and traffic modeling. He has authored two books: *Switching Theory, Architectures and Performance in Broadband ATM Networks* (New York: Wiley, 1998) and *Communication Networks* (McGraw-Hill, 2002, in Italian).

Dr. Pattavina has been an Editor for switching architecture performance of the IEEE TRANSACTIONS ON COMMUNICATIONS since 1994 and Editor-in-Chief of the *European Transactions on Telecommunications* since 2001. He is a Senior Member of the IEEE Communications Society.



Diego Carzaniga was born in Milano, Italy, in 1980. He received the Dr. Ing. degree in telecommunications engineering from the Politecnico di Milano, in 2005.

Since 2005, he has been involved in SIP software development in private industry.



Alessandro Antonino was born in Benevento, Italy, in 1978. He received the degree in electronic engineering from the Politecnico di Torino, Torino, Italy, in 2006.

He is an Assistant Professor with Politecnico di Torino.